CSIRO PUBLISHING
www.publish.csiro.au/journals/fpb *Functional Plant Biology*, 2008, **35**, 553–564

Deactivation of aquaporins decreases internal conductance to CO_2 diffusion in tobacco leaves grown under long-term drought

Shin-Ichi Miyazawa[A], *Satomi Yoshimura*[A], *Yuki Shinzaki*[A], *Masayoshi Maeshima*[B] *and Chikahiro Miyake*[A,C,D]

[A]Research Institute of Innovative Technology for the Earth (RITE), 9-2 Kizugawadai, Kizugawa City, Kyoto 619-0292, Japan.
[B]Laboratory of Cell Dynamics, Graduate School of Bioagricultural Sciences, Nagoya University, Nagoya 464-8601, Japan.
[C]Present address: Laboratory of Plant Nutrition, Department of Biological and Environmental Science, Faculty of Agriculture, Graduate School of Agricultural Science, Kobe University, Nada, Kobe 657-8501, Japan.
[D]Corresponding author. Email: cmiyake@hawk.kobe-u.ac.jp

Abstract. We compared the diffusion conductance to CO_2 from the intercellular air space to the chloroplasts (internal conductance (g_i)) between tobacco leaves acclimated to long-term drought (drought-acclimated (DA)) and those grown under sufficient irrigation (well-watered (WW)), and analysed the changes in g_i in relation to the leaf anatomical characteristics and a possible CO_2 transporter, aquaporin. The g_i, which was estimated by combined analyses of CO_2 gas exchange with chlorophyll fluorescence, in the DA plants was approximately half of that in the WW plants. The mesophyll and chloroplast surface areas exposing the intercellular air space, which potentially affect g_i, were not significantly different between the WW and DA plants. The amounts of plasma membrane aquaporins (PIP), immunochemically determined using radish PIP antibodies, were unrelated to g_i. After treatment with $HgCl_2$, an aquaporin inhibitor, the water permeability of the leaf tissues (measured as the weight loss of fully-turgid leaf disks without the abaxial epidermis in 1 M sorbitol) in WW plants decreased with an increase in $HgCl_2$ concentration. The g_i in the WW plants decreased to similar levels to the DA plants when the detached leaflets were fed with 0.5 mM $HgCl_2$. In contrast, both water permeability and g_i were insensitive to $HgCl_2$ treatments in DA plants. These results suggest that deactivation of aquaporins is responsible for the significant reduction in g_i observed in plants growing under long-term drought.

Additional keywords: acclimation, drought stress, leaf anatomy, mesophyll conductance.

Introduction

The net photosynthesis rate on a leaf-area basis (A) generally decreases in drought-acclimated (DA) leaves of C_3 plants. These reductions in A are partly attributed to decreases in the chloroplastic CO_2 concentration (C_c) because both stomatal conductance to water vapour (g_s) and diffusion conductance to CO_2 from the intercellular air space to the chloroplasts (internal conductance (g_i)) significantly decrease in DA plants (Galmes *et al*. 2006; Monti *et al*. 2006). In contrast, the water-use efficiency (WUE = A per unit transpiration rate) increases in DA leaves, and this has been reported for some C_3 species, including *Ulmus americana* L. (Reich *et al*. 1989) and *Helianthus annuus* L. (Fredeen *et al*. 1991). The transpiration rate decreases more rapidly than A with a decrease in g_s, such that the DA plants have a higher WUE than well-watered (WW) plants (Lambers *et al*. 1998; Nobel 1999). In contrast, the physiological importance of g_i to drought adaptation is not clearly understood (Flexas *et al*. 2008; Warren 2008).

As shown in previous studies (Evans *et al*. 1994; Terashima *et al*. 2001), g_i is composed of liquid-phase conductance (g_{liq}) and gas-phase conductance (g_{gas}):

$$g_i = \frac{g_{liq}}{1 + \frac{g_{liq}}{g_{gas}}}. \quad (1)$$

g_{liq} is expressed as $g'_{liq}\,S_c$, where S_c and g'_{liq} represent the chloroplast surface area facing the intercellular air space and the liquid-phase conductance per unit S_c, respectively. Thus, Eqn (1) is given as:

$$g_i = \frac{g'_{liq} S_c}{1 + \frac{g'_{liq} S_c}{g_{gas}}}. \quad (2)$$

g_{gas} depends on the mesophyll thickness and the fraction of the mesophyll volume occupied by the intercellular air space (f_{ias}). g'_{liq} is affected by both the thickness and the properties of the pathways from the mesophyll cell surfaces to the active sites of

© CSIRO 2008
10.1071/FP08117 1445-4408/08/070553

Rubisco (Hanba *et al*. 1999; Miyazawa and Terashima 2001; Terashima *et al*. 2005). g_{gas} cannot be a major limitation for the net photosynthesis rates, particularly in amphistomatous leaves, such as tobacco leaves, because CO_2 diffuses ~10^4-fold faster in the gas-phase than in the liquid-phase (Parkhurst and Mott 1990; Evans *et al*. 1994). Thus, Eqn (2) is approximated by $g_i = g'_{liq} S_c$. S_c is close to the mesophyll surface area facing the intercellular air space (S_{mes}) when the chloroplasts occupy most of the S_{mes}. Therefore, g_i is roughly proportional to S_{mes} (Syvertsen *et al*. 1995; Terashima *et al*. 2005). The anatomical characteristics of leaves change in response to long-term drought and might affect g_i (Chartzoulakis *et al*. 2002).

A number of recent studies have revealed that aquaporins are proteins that might regulate g'_{liq} (Terashima and Ono 2002; Hanba *et al*. 2004; Flexas *et al*. 2006). Aquaporins have originally been known as proteins that facilitate and regulate water transport across biological membranes. Water transport by aquaporins occurs in a manner dependent on the osmotic pressure and water potential gradient. Some members of the aquaporin family transport CO_2 molecules; this was shown for *Xenopus* oocytes expressing a human aquaporin (AQP1, Cooper and Boron 1998; Nakhoul *et al*. 1998; but see Yang *et al*. 2000) or a tobacco plasma membrane aquaporin (NtAQP1, Uehlein *et al*. 2003). g_i decreased when $HgCl_2$, an aquaporin inhibitor, was fed to the petioles of *Vicia faba* L. and *Phaseolus vulgaris* L. leaves (Terashima and Ono 2002). Furthermore, Hanba *et al*. (2004) indicated that transgenic rice plants overexpressing the barley plasma membrane aquaporin HvPIP2;1 had larger g_i than wild-type plants. Transgenic tobacco (*Nicotiana tabacum* L.) plants overexpressing and suppressing NtAQP1 had higher and lower g_i, respectively, than their respective wild-type plants (Flexas *et al*. 2006). These studies have clearly demonstrated that plasma membrane aquaporins regulate g_i.

Plasma membrane aquaporins are classified into two subfamilies; PIP1 and PIP2. Each subfamily has several isoforms in radish (Suga *et al*. 2001) and in *Arabidopsis thaliana* L. (Johanson and Gustavsson 2002). Suga and Maeshima (2004) measured aquaporin activity with a stopped-flow spectrophotometer using the membrane vesicles of the yeast cells expressing radish plasma membrane aquaporins, and demonstrated that PIP2s generally have a much higher water transport activity than PIP1s. As the vesicles were incubated with 5 mM $HgCl_2$, the activities of PIP2s were severely inhibited while those of PIP1s were relatively insensitive to the mercury treatments. A PIP2-type aquaporin identified in spinach (PM28A) is phosphorylated in response to an increase in apoplastic water potential; this was demonstrated using leaf pieces infiltrated with media containing labelled phosphate and different concentrations of sucrose (Johansson *et al*. 1996). The water transport activity of PM28A decreases as a result of the de-phosphorylation of the cytoplasmic sites of the aquaporins (Johansson *et al*. 1998). Thus, the mercury sensitivity of the water-transport activities differs among the aquaporin isoforms and the water-transport activity of the aquaporins is probably regulated by phosphorylation in response to the cellular water balance.

Transgenic studies have clearly shown that aquaporin plays a pivotal role in regulating g_i. In contrast, there is little information on the physiological mechanisms responsible for the significant reductions in g_i in DA leaves. In tobacco plants intermittently irrigated (DA) or sufficiently irrigated (WW), we addressed questions aiming to clarify the underlying mechanisms by which both leaf anatomical characteristics and leaf aquaporins affect g_i.

Materials and methods

Growth conditions

Tobacco (*Nicotiana tabacum* L. cv. Xanthi) plants were grown in 0.7-L pots filled with peat-moss-based soils. Six pots, each with one plant, were placed on a 4-L tray. The plants were supplied with a 1000-fold diluted commercial fertiliser (Hyponex 6–10–5; Hyponex Japan, Osaka, Japan). In addition, 2 L of the fertiliser was applied to each tray every 2 weeks until four true leaves appeared. Thereafter, 2 L of the fertiliser was supplied to each tray intermittently (every 4 days) for raising the DA plants and every 1–2 days for the WW plants. The treatments were continued for 2–3 weeks until the developing leaves were fully expanded.

The leaves were grown under a PPFD of ~850 μmol m^{-2} s^{-1}, a relative humidity of 60/50% (day/night) and a temperature of 25/22°C (day/night) in an environmentally controlled growth chamber. The volumetric soil water content was measured with a soil moisture sensor (ECH2O probe model EC-5; Decagon Devices, Pullman, WA, USA). Fully-expanded mature leaves were used. For all measurements, except for the measurement of soil water content, we used at least three plants from each treatment. All measurements on DA leaves were carried out 1 or 2 days later when the plants were supplied with the fertiliser.

Measurement of photosynthesis

Photosynthesis measurements were carried out with a portable CO_2 exchange analyser combined with a chlorophyll fluorometer (LI-6400; Li-Cor, Lincoln, NE, USA). To minimise CO_2 leakage from the chamber, the gaskets were surrounded by a laboratory-made skirt with which the air once exhausted from the chamber was again blown to the outer surface of the gaskets. The gas exchange analyser was linked with a gas cylinder containing either 20% or 2% O_2 balanced in N_2. A dew point generator (LI-610; Li-Cor) was placed in between the analyser and the cylinders to saturate the gases supplied from the cylinders with water vapour. The temperature of the dew point generator was set between 14 and 17°C.

When measuring photosynthesis, the plants were taken from the growth chamber before the lights were switched on and were supplied with enough water to saturate the soil. First, the dark respiration rate was measured at a CO_2 concentration surrounding the leaves (C_a) of 360 μmol mol^{-1}. The net photosynthesis rate on a leaf-area basis (A) at $C_a = 360$ μmol mol^{-1} reached steady-state levels 20–30 min after the red/blue LED lights of the analyser had been turned on. The changes in A against the CO_2 concentration of the intercellular air space (C_i), that is, A–C_i responses, were generated by stepwise changes in the supplied CO_2 concentrations. The leaf temperature, incident PPFD and leaf to air vapour pressure deficit were 25°C, 1000 μmol m^{-2} s^{-1} and 0.9–1.2 kPa, respectively.

Calculation of g_i by the chlorophyll-fluorescence method

The CO_2 concentration in the chloroplast (C_c) was calculated as:

$$C_c = \frac{O_c V_c}{\tau V_o}, \quad (3)$$

where O_c is the chloroplastic O_2 concentration, τ is the relative specificity of Rubisco, and V_c and V_o are the carboxylase and oxygenase rates of Rubisco. O_c was assumed to be 200 mmol mol^{-1}. τ was assumed to be 2665 mol mol^{-1} at 25°C, which was based on *in vitro* measurements for *N. tabacum* leaves (von Caemmerer 2000; Galmes *et al*. 2006).

V_c and V_o were calculated from both the CO_2 gas exchange rate and the electron transport rate (J) on the basis of the NADPH consumption rate for the photosynthetic carbon reduction and oxidation cycles. V_c and V_o were given as:

$$V_c = \frac{1}{6}\left[\frac{J}{2} + 4(A + R_d)\right] \quad (4)$$

and

$$V_o = \frac{1}{6}[J - 4(A + R_d)], \quad (5)$$

where R_d is the rate of mitochondrial respiration in light. R_d was assumed to be half of the dark respiration rate (Atkin *et al*. 1998; Yamori *et al*. 2006).

J was approximated by the following equation:

$$J = \alpha\beta I(\Phi PSII), \quad (6)$$

where α is the absorptance of the leaf, β is the fraction of absorbed irradiance that reaches PSII, I is the incident irradiance, and ΦPSII is the quantum yield of PSII. α was measured with a quantum sensor equipped with an integration sphere (LI-1800, Li-Cor). β was calculated from both the CO_2 gas exchange rates and the electron transport rates measured under moderate PPFD (300 µmol m^{-2} s^{-1}) and non-photorespiratory conditions (2% O_2 and 2000 µmol mol^{-1} CO_2). ΦPSII was determined with chlorophyll fluorescence (Genty *et al*. 1989).

g_i was calculated as:

$$g_i = \frac{k_c k_i}{k_c - k_i}, \quad (7)$$

where k_i and k_c represent the initial slopes of the A–C_i and A–C_c curves, respectively. The initial slopes were obtained from linear regression analysis carried out using values of C_i that were <200 µmol mol^{-1}.

Calculation of g_i by the curve-fitting method

An estimation of g_i by the chlorophyll-fluorescence method is based on an assumption that J is not required by processes such as the Mehler reaction, the nitrogen assimilation cycle and cyclic electron flow around PSII (Epron *et al*. 1995; Miyake and Okamura 2003). In addition, g_i was calculated using the curve-fitting procedure developed by Ethier and Livingston (2004), which is independent of the validity of J. The curve-fitting procedure is based on an assumption that a decrease in g_i reduces the curvature of the Rubisco-limited portion of the A–C_i curve. Under Rubisco-limited conditions, A is given as:

$$A = \frac{-b + \sqrt{b^2 - 4ac}}{2a}$$

$$a = -1/g_i$$

$$b = (V_{cmax} - R_d)/g_i + C_i + K_c(1 + O_c/K_o)$$

$$c = R_d[C_i + K_c(1 + O_c/K_o)] - V_{cmax}(C_i - \Gamma^*), \quad (8)$$

where V_{cmax} is the maximal Rubisco carboxylation rate, K_c and K_o are the Michaelis–Menten constants of Rubisco for CO_2 and O_2, respectively, and Γ^* is the chloroplastic CO_2 compensation point. Eqn (8) was fitted to the Rubisco-limited portion of the A–C_i curves (C_i, <200 µmol mol^{-1}). K_c $(1 + O_c/K_o)$ and Γ^* were assumed to be 601 µmol mol^{-1} and 38 µmol mol^{-1}, respectively (Bernacchi *et al*. 2002). R_d was assumed to be half of the dark respiration rate. The curve-fitting procedure was carried out with non-linear least-square fits (Levenberg–Marquardt algorithm). R_d was fixed when fitting the data.

Measurement of the Rubisco, water-soluble protein, chlorophyll and nitrogen contents

After the photosynthesis measurement experiments, leaf disks were collected from the lamina, excluding the midribs, and were stored in a freezer at −80°C. The leaf materials (two leaf disks per sample) were ground in 0.75 mL of buffer containing 50 mM potassium phosphate (pH 7.4), 10 mM sodium ascorbate, 10 mM EDTA and 1% (w/v) polyvinylpyrrolidone with a tablet of protease inhibitor cocktail (Nacalai Tesque, Kyoto, Japan) followed by mild centrifugation (×600*g* for 5 min at 4°C). The soluble protein content in the supernatant (water-soluble protein content) was determined using a protein assay reagent and BSA as a standard (Protein Assay CBB solution; Nacalai Tesque). The supernatant was mixed with 2× Laemmli buffer consisting of 125 mM Tris–HCl (pH 6.8), 4% (w/v) SDS, 10% (v/v) β-merchaptoethanol, 20% (v/v) glycerol and 0.01% (w/v) bromphenol blue. The mixture was heated at 90°C for 5 min and was subjected to SDS–PAGE. The SDS gel was stained with Coomassie Brilliant Blue R-250.

According to the method described by Makino *et al*. (1986), the stained bands corresponding to the Rubisco large subunits were eluted using formamid, and the Rubisco content was determined spectrophotometrically using BSA as a standard. Rubisco content on a leaf-area basis was expressed as a value relative to the highest Rubisco content found in the present study. The chlorophyll from the leaf disks was extracted with *N*, *N*-dimethylformamide, and its content was determined spectrophotometrically (Porra *et al*. 1989). The total nitrogen content of the leaf disks was determined by the Kjeldahl digestion method (SuperKjel 1200/1250; ACTAC, Tokyo, Japan).

Measurement of aquaporin content

Western blotting was carried out using antibodies to radish plasma membrane aquaporins (anti-all PIPs and anti-PIP2s). The details of the antibodies have been described previously by Ohshima *et al*. (2001) and Suga and Maeshima (2004). The

anti-all PIPs were prepared using a conserved sequence of all the isoforms of the plasma membrane aquaporins in the N-terminal region (KDYNEPPPAPLFEPGELSSWS) as an antigen peptide. The anti-PIP2s were prepared using a conserved sequence among the PIP2s isoforms in the C-terminal region (QFVLRASGSKSLGSFRSA) as an antigen peptide.

Aquaporins are highly hydrophobic proteins and are present in oligomeric forms *in planta*. The oligomeric forms are observed on SDS–PAGE, in particular when the proteins are dissociated from the membranes at a high temperature (Maeshima 1992). We carefully chose the dissociation protocol to prevent the aquaporins from forming the oligomers on SDS–PAGE. According to the method described by Maeshima (1992), the supernatant mixed with the Laemmli buffer was heated at 70°C for 5 min and was subjected to SDS–PAGE.

The resolved proteins were transferred onto polyvinylidene difluoride membranes (Hybond-P; GE Healthcare, Buckinghamshire, UK). The membranes were blocked with 5% de-fatted milk before reaction with the primary antibody. The blots were visualised using horseradish-coupled protein A and chemifluorescence reagents (ECL Advance western blotting Detection Kit; GE Healthcare). Images were obtained with an image analyser (LAS-3000; FUJIFILM, Tokyo, Japan). Bands near 30 kD, which correspond to plasma-membrane aquaporins in the monomeric form, were scanned with computer software (Multi Gauge ver 2.0; FUJIFILM). The number of pixels for each sample was determined and expressed as a value relative to that of the highest g_i found in the present study.

Leaf anatomy

Leaf pieces (~1 mm × 3 mm; major veins avoided) were cut from the middle parts of the lamina with a razorblade. The pieces were fixed in 100 mM phosphate buffer (pH 7.2) containing 2.0% glutaraldehyde for at least 6 h at 4°C after vacuum infiltration and were post-fixed in 2% osmium tetroxide for 3 h. The pieces were dehydrated in an acetone and propylene oxide series, and were embedded in Quetol 651 resin (Nisshin EM, Tokyo, Japan). Leaf transverse sections (1 μm in thickness) were obtained using a microtome (RM2245; Leica Microsystems, Wetzler, Germany) and were stained with 0.5% toluidine blue. The sections were photographed with a digital camera linked to a microscope (BX50; Olympus, Tokyo, Japan).

S_{mes}, f_{ias}, the S_c/S_{mes} ratio and the thicknesses of the leaf, mesophyll tissue and upper and lower epidermises were measured on light micrographs using a digitising pad (Evans *et al*. 1994; Syvertsen *et al*. 1995; Miyazawa and Terashima 2001). To convert the lengths into surface area, curvature correction factors for the palisade and spongy tissues were obtained, assuming that the cells where spheroid in shape (Thain 1983).

Water permeability of leaf tissues

Water permeability of the leaf tissues was measured according to the method described by Terashima and Ono (2002). The abaxial epidermis was removed from the leaf disks (diameter 15 mm) using a pair of tweezers. The leaf disks were floated on 20 mL of distilled water in a Petri dish for more than 10 min with the adaxial surface facing upwards. Excess water on the leaf disks was absorbed using a piece of Kimwipe paper, and the disks were immediately weighed (initial FW (iFW)). The disks were floated on 20 mL of $HgCl_2$ solution in a Petri dish for a further 5 min and were subsequently floated on 20 mL of 1 M sorbitol solution for 60 s. The disks were immediately weighed again (dehydrated FW (dFW)). The adaxial surfaces always faced upwards when the leaf disks were floated on the solutions. Before weighing the leaf disks, the excess solution on the disks was absorbed using a piece of Kimwipe paper. The relative water loss was calculated as (iFW – dFW)/iFW.

$HgCl_2$ feeding

Fully-expanded, mature leaves were detached from the plants using a pair of scissors. The petioles were immediately immersed

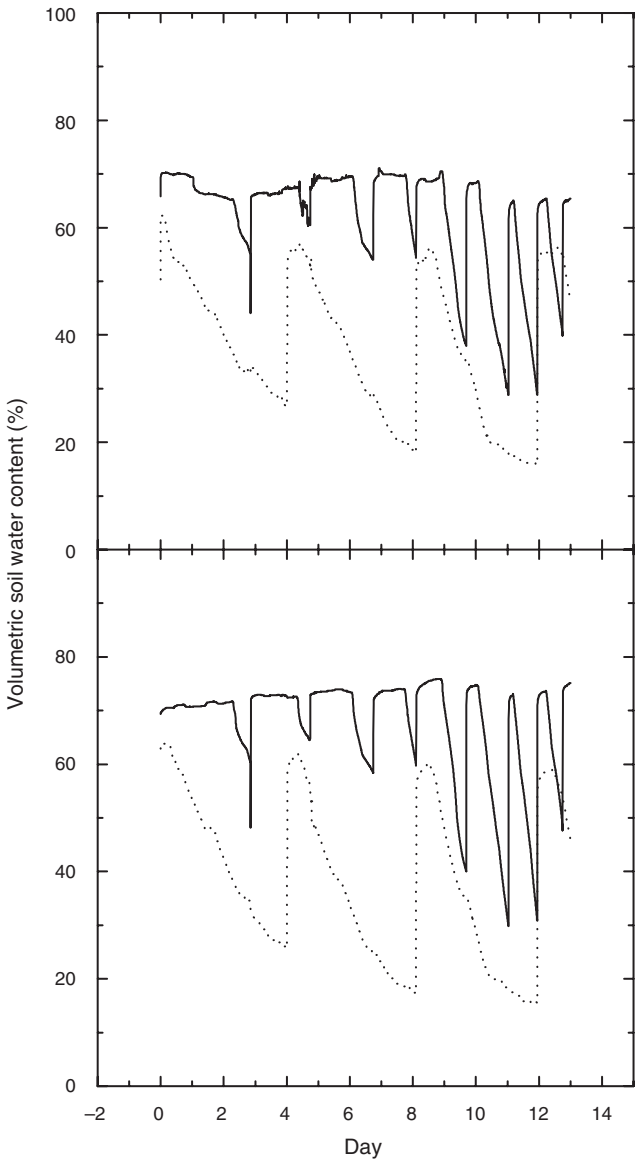

Fig. 1. Changes in volumetric soil water content in well-watered (solid lines) and drought-acclimated (dotted lines) tobacco plants. Data from the two different pots (upper and lower panels) are shown for each treatment.

in Falcon tubes filled with 50 mL distilled water, and the bases of the petioles were cut again in distilled water. After obtaining the A–C_i curves, C_a was returned to 360 μmol mol^{-1}. Subsequently, 250 mM $HgCl_2$ was added to the tubes. The final concentration of $HgCl_2$ in the tubes was 0.5 mM. The data were automatically logged at an interval of 5 min after $HgCl_2$ treatment. A–C_i responses were obtained again at 2.5–3.0 h after $HgCl_2$ feeding.

Statistical analysis

All statistical analyses were carried out using the software package SPSS 14.0 (SPSS, Chicago, IL, USA).

Results

Soil water content

The volumetric soil water content fluctuated during the treatments (Fig. 1). In the drought treatments, the soil water content gradually decreased and levelled off at ~20% at 4 days after sufficient irrigation. The leaves of the plants subjected to drought wilted when the soil water content reached this level. The leaves recovered completely on the days after irrigation. In contrast, under WW conditions, the soil water content did not decrease to such low levels. The soil water content tended to fluctuate more sharply as plant size increased.

Changes in the photosynthetic characteristics in response to long-term drought

The maximum quantum yield of PSII (F_v/F_m) in the DA plants was ~0.8, indicating that the photosynthetic machinery in these plants was not severely damaged by the drought treatment. There were no significant differences in the leaf absorptance (α), the fraction of irradiance that reaches PSII (β), and the dark respiration rate on a leaf-area basis between the plants (Table 1). As shown by the A–C_i and A–C_c responses, the net photosynthesis rate on a leaf-area basis (A) and the

Table 1. The maximum quantum yield of PSII (F_v/F_m), leaf absorptance (α), fraction of absorbed irradiance that reaches PSII (β), and dark respiration rate on a leaf-area basis in well-watered and drought-acclimated tobacco plants

Data are mean ± s.d. of 6–7 sample leaves. P indicates the significance value of the t-tests between well-watered and drought-acclimated plants

	Well-watered	Drought-acclimated	P
F_v/F_m	0.841 ± 0.014	0.825 ± 0.013	0.043
α	0.837 ± 0.010	0.830 ± 0.008	0.206
β	0.538 ± 0.017	0.54 ± 0.03	0.779
Dark respiration rate	1.7 ± 0.5	1.2 ± 0.5	0.070

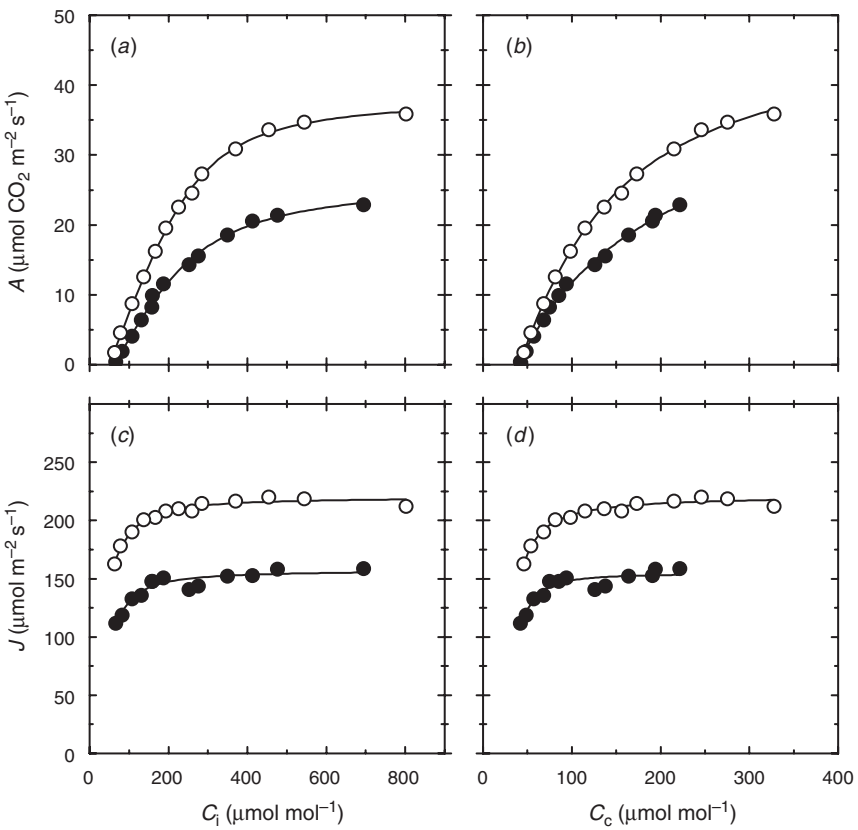

Fig. 2. Changes in net photosynthesis rate (A) and electron transport rate (J) against CO_2 concentration in the substomatal cavities (C_i) and against the CO_2 concentration in the chloroplasts (C_c) in well-watered (○) and drought-acclimated (●) tobacco. C_c was calculated by the chlorophyll fluorescence method. The calculated internal conductance to CO_2 (g_i) is shown in Table 2. Data are represented as the mean of seven sample leaves. Non-rectangular hyperbolic curves were fitted to the data.

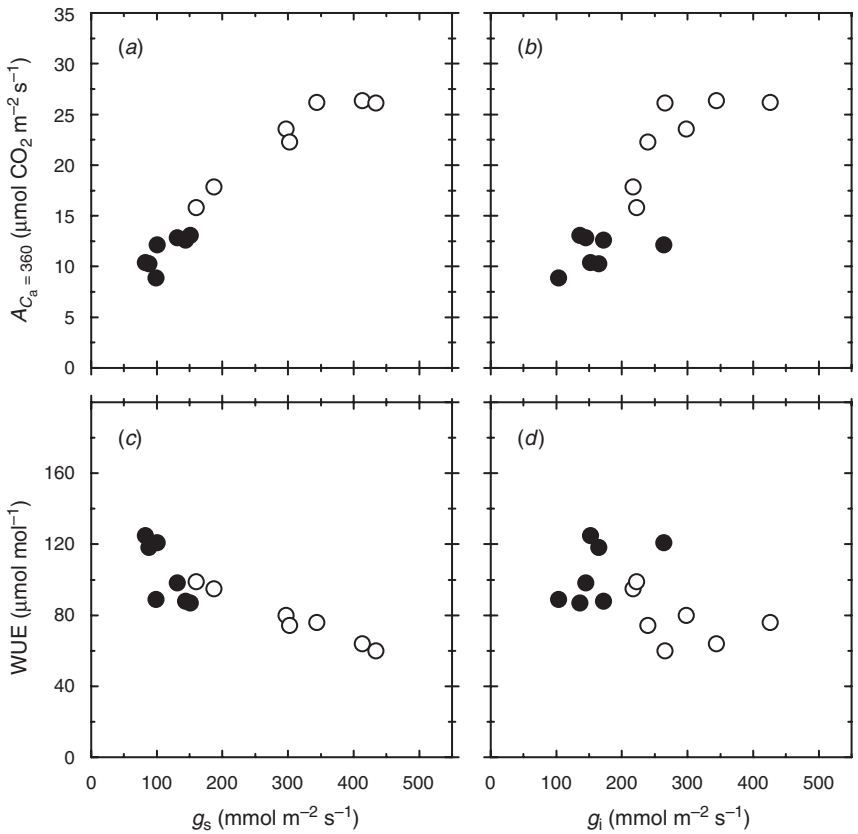

Fig. 3. Changes in net photosynthesis rate on a leaf-area basis ($A_{C_a=360}$) and water-use efficiency (WUE), both of which were measured at an ambient CO_2 concentration of 360 μmol mol^{-1}, against stomatal conductance to water vapour (g_s) or internal conductance to CO_2 (g_i) in well-watered (○) and drought-acclimated (●) tobacco plants. g_s was measured under ambient CO_2 concentration. g_i was calculated by the chlorophyll fluorescence method. WUE is defined as $A_{C_a=360}$ divided by the corresponding g_s.

electron transport rate (J) significantly decreased when the leaves were acclimated to long-term drought (Fig. 2). On average, the net photosynthesis rate measured at ambient CO_2 concentration (i.e. $A_{C_a=360}$) in the DA leaves was approximately half of that in the WW leaves (Fig. 3), and the WUE in the DA leaves was, on average, 30% higher than that in the WW leaves.

The average g_i values calculated by the chlorophyll-fluorescence method agreed with those calculated by the curve-fitting method (Table 2); hence, we used the g_i values calculated by the chlorophyll-fluorescence method for further analyses. On average, g_s in the DA leaves was approximately

Table 2. Comparison of the calculated internal conductance to CO_2 diffusion (g_i) in tobacco plants determined by the chlorophyll fluorescence method and the curve-fitting method

Data are the mean ± s.d. of seven sample leaves for each treatment. P indicates the significance value of t-tests between the two methods in each treatment

	g_i (mmol m^{-2} s^{-1})		
	Chl. fluorescence method	Curve-fitting method	P
Well-watered	290 ± 80	340 ± 160	0.474
Drought-acclimated	160 ± 50	150 ± 40	0.543

Table 3. Photosynthetic gas exchange parameters (C_i, C_c/C_i ratio and initial slopes of A–C_i and A–C_c responses) and the area-based contents of Rubisco, water-soluble protein, chlorophyll and nitrogen for well-watered and drought-acclimated tobacco leaves

C_i, CO_2 concentration in the substomatal cavities; C_c, CO_2 concentration in the chloroplasts; k_i, initial slope of the A–C_i response; k_c, initial slope of the A–C_c response. C_i and C_c/C_i ratio were measured at an ambient CO_2 concentration of 360 μmol mol^{-1}. C_c was calculated by the chlorophyll fluorescence method. The Rubisco content on a leaf-area basis was expressed as a relative value to the largest Rubisco content observed in the present study. Data are the mean ± s.d. of seven sample leaves. P indicates the significance value of t-tests between well-watered and drought-acclimated plants

	Well-watered	Drought-acclimated	P
C_i (μmol mol^{-1})	230 ± 20	190 ± 30	0.012
C_c/C_i ratio	0.60 ± 0.06	0.51 ± 0.07	0.019
k_i (mol m^{-2} s^{-1})	0.135 ± 0.017	0.091 ± 0.014	<0.001
k_c (mol m^{-2} s^{-1})	0.263 ± 0.011	0.20 ± 0.03	0.002
Rubisco content (relative value)	0.79 ± 0.16	0.77 ± 0.10	0.797
Water-soluble protein content (g m^{-2})	6.7 ± 0.6	6.5 ± 0.3	0.408
Chlorophyll content (μmol m^{-2})	420 ± 60	373 ± 16	0.072
Nitrogen content (g m^{-2})	1.5 ± 0.3	1.8 ± 0.3	0.057

one-third of that in the WW leaves (Fig. 3). The decrease in g_i was of a smaller magnitude compared with the changes in g_s. The decreases in g_s and g_i resulted in low C_i and low C_c/C_i ratios, respectively (Table 3).

As shown in Table 3, the area-based amounts of Rubisco, soluble protein, chlorophyll and nitrogen did not differ significantly between the treated leaves. In contrast, the initial slope of the A–C_c response, which is closely coupled with the Rubisco carboxylation capacity, was lower in the DA than that in the WW leaves. Taken together, these results indicate that significant reductions in $A_{C_a=360}$ in the DA leaves result from both low C_c and low activity of Rubisco.

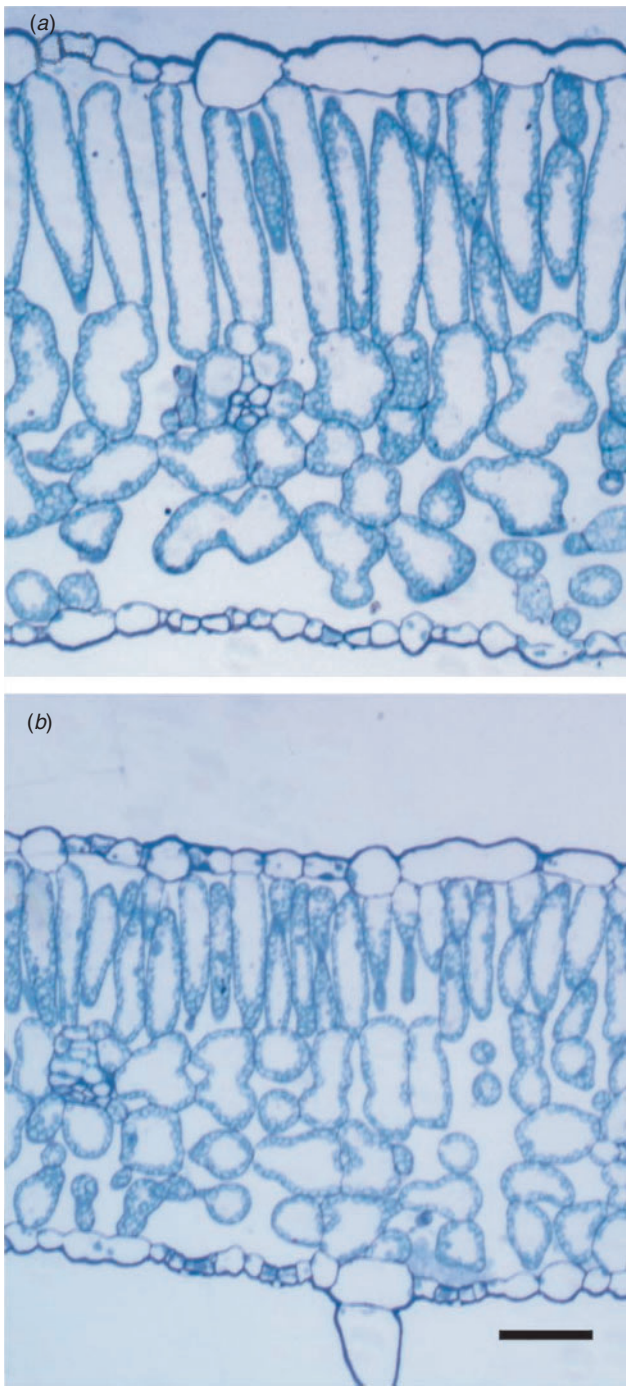

Fig. 4. Light micrographs of transverse sections of (*a*) well-watered and (*b*) drought-acclimated tobacco leaves. Scale bar = 50 μm.

Changes in leaf anatomical characteristics

Total leaf thickness was reduced when the leaves were acclimated to long-term drought (Fig. 4; Table 4). This decrease in total leaf thickness was accompanied by a decrease in mesophyll tissue thickness. There were no significant differences in the mesophyll surface area exposing the intercellular air space (S_{mes}) or in the fraction of mesophyll volume occupied by the intercellular air space (f_{ias}) between the DA and WW leaves. The S_c/S_{mes} ratio in the DA leaves was similar to that in the WW leaves. Together with the S_{mes} data, this result indicates that the chloroplast surface area (S_c) did not differ much between the treated leaves. The mesophyll cell density in the DA leaves tended to be higher than that in the WW leaves.

Changes in leaf aquaporin contents

Major bands larger than 30 kDa, which corresponds to the size of the monomers, were not detected using the anti-all PIPs or the anti-PIP2s in the leaves. Overall, the total plasma membrane aquaporin (all PIPs) content on a leaf-area basis was slightly lower in the DA leaves than in the WW leaves (Fig. 5). The relationships between g_i and all PIP contents on a leaf-area basis were obscure in both the WW plants ($r = -0.64$, $P = 0.12$) and in the DA plants ($r = -0.17$, $P = 0.72$). When all the data from both treatments were pooled, we did not find a significant correlation either ($r = 0.21$, $P = 0.46$). The protein levels of mercury-sensitive aquaporin isoforms (PIP2s) in the DA leaves were comparable to those in the WW leaves (Fig. 6). Interestingly, the electrophoretic mobility of the PIP2s in the DA plants increased slightly.

Effects of $HgCl_2$ on the water permeability of the leaf tissues and g_i

In the WW plants, the water permeability of the leaf tissues decreased by ~20% with treatment with 0.5 mM $HgCl_2$ and it remained unchanged with treatment with >0.5 mM $HgCl_2$ (Fig. 7*a*). In contrast, the water permeability of the DA

Table 4. Anatomical characteristics of the leaves of well-watered and drought-acclimated tobacco plants

S_{mes}, mesophyll surface area facing the intercellular air space, which is expressed on a leaf-area basis; S_c/S_{mes} ratio, ratio of chloroplast surface area to S_{mes}; f_{ias}, fraction of mesophyll volume occupied by the intercellular air space. Data are the mean ± s.d. of nine sample leaves for each treatment, except for the S_c/S_{mes} ratio (five sample leaves). P indicates the significance value of t-tests between well-watered and drought-acclimated leaves

	Well-watered	Drought-acclimated	P
Thickness (μm)			
Total leaf	320 ± 20	270 ± 30	0.002
Mesophyll tissue	280 ± 30	240 ± 20	0.003
Upper epidermis	23 ± 2	20 ± 4	0.058
Lower epidermis	17 ± 2	16 ± 2	0.768
S_{mes} ($m^2\ m^{-2}$)	21 ± 3	21.4 ± 1.7	0.915
S_c/S_{mes} ratio	0.88 ± 0.04	0.91 ± 0.03	0.209
f_{ias} (%)	29 ± 2	26 ± 5	0.132

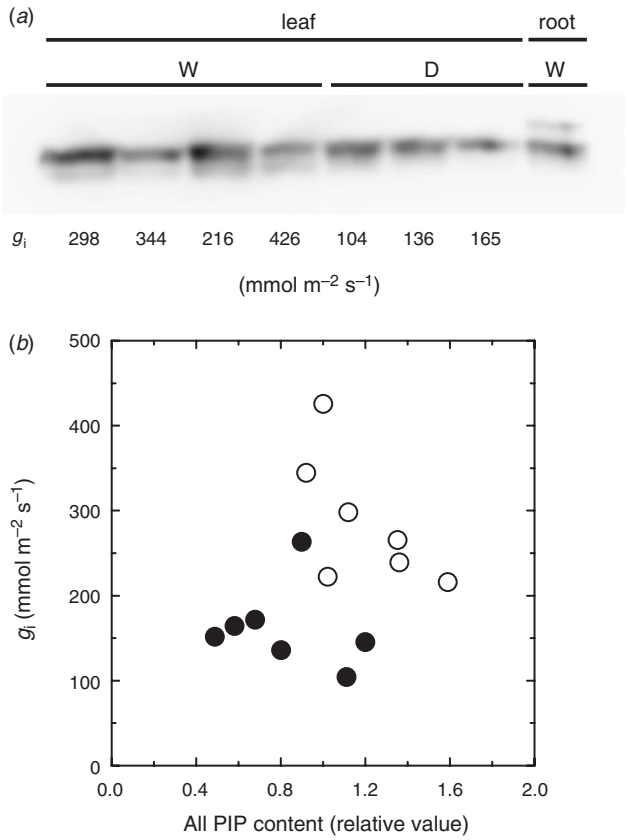

Fig. 5. (*a*) Protein levels of total plasma membrane aquaporins (all PIPs) in tobacco leaves and roots. W, well-watered; D, drought-acclimated. For leaves and roots, 40 µg and 2.5 µg of water-soluble proteins, respectively, were loaded into each lane. The internal conductance to CO_2 (g_i) is shown below the corresponding bands. (*b*) Relationship between g_i and all PIP contents on a leaf-area basis in well-watered (○) and drought-acclimated (●) tobacco. g_i was calculated by the chlorophyll fluorescence method. All PIP were immunochemically determined using the radish anti-all PIPs. The amount of all PIPs for each sample is expressed as a value relative to that of the highest g_i observed in the present study.

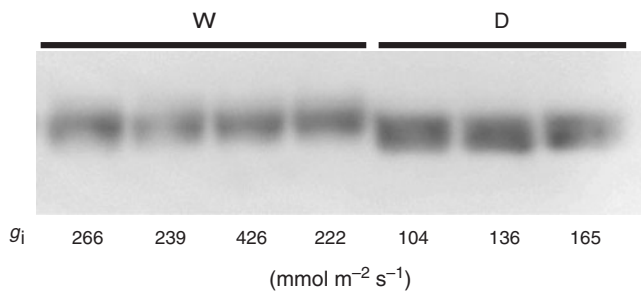

Fig. 6. Protein levels of mercury-sensitive plasma membrane aquaporins (PIP2s) were immunochemically determined using radish anti-PIP2s in well-watered (W) and drought-acclimated (D) tobacco leaves. Water-soluble proteins (20 µg) were loaded into each lane. The internal conductance to CO_2 (g_i) is shown below the corresponding bands.

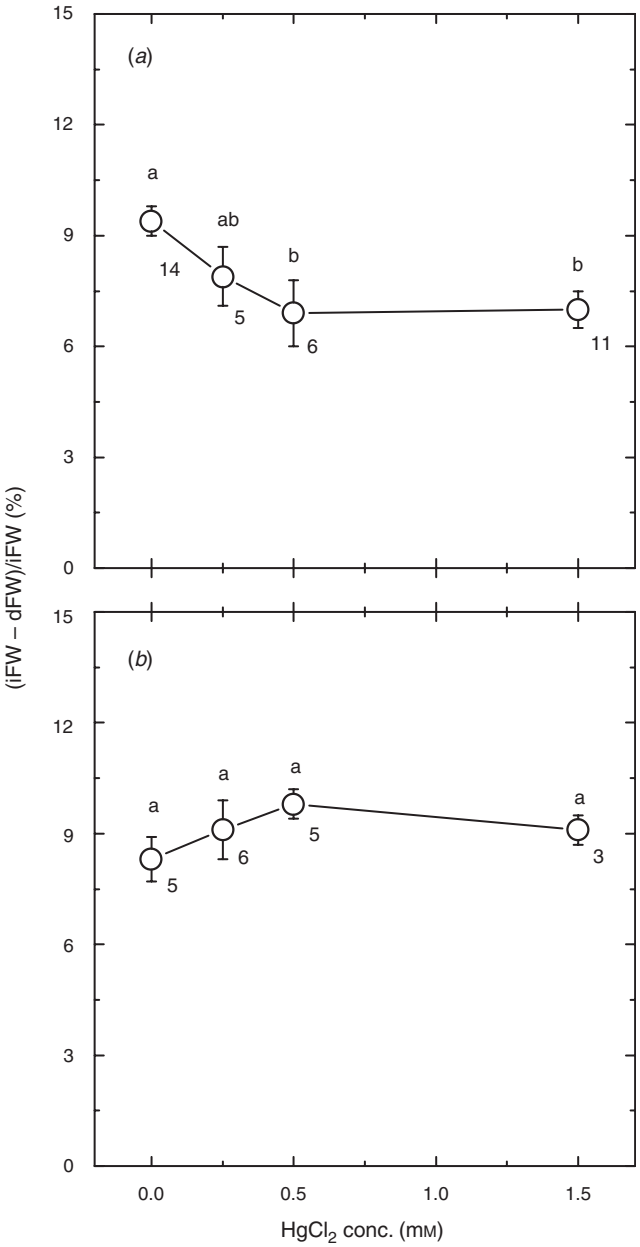

Fig. 7. Effects of $HgCl_2$ on the water permeability of leaf disks without the abaxial epidermis in (*a*) well-watered and (*b*) drought-acclimated tobacco plants. Fully turgid leaf disks without the abaxial epidermis were treated with $HgCl_2$ solutions and weighed (initial FW (iFW)). Subsequently, the leaf disks were dehydrated in 1 M sorbitol solution for 60 s, and reweighed (dehydrated FW (dFW)). The iFW values were 49 ± 6 mg (n = 36, mean ± s.d.) and 45 ± 5 mg (n = 19) for well-watered and drought-acclimated leaves, respectively. Weight loss relative to the initial weight was calculated. A Sheffe's test was used to evaluate the significant difference between the results of the mercury treatments. Data are represented as the means ± s.e. of 3–14 leaf disks. The number of sample leaf disks taken for each treatment is shown beside each plot. Different letters denote the mean significant difference at $P < 0.05$ for each treatment.

plants remained almost constant at all concentrations of mercury (Fig. 7*b*).

As shown in Fig. 8, the initial slope of the A–C_i response in the WW leaflets decreased markedly when 0.5 mM $HgCl_2$ was fed to the petioles ($P < 0.01$, t-test). Moreover, A at C_i >200 μmol mol^{-1} was lowered by $HgCl_2$ feeding to the WW leaflets, implying that the regeneration rate of ribulose-1, 5-bisphosphate was retarded owing to inhibitions of plastocyanin and Calvin cycle enzymes that contain sulfhydryl groups (Terashima and Ono 2002). However, the Rubisco carboxylation capacities would remain unaffected because the initial slopes of the A–C_c responses did not change even after $HgCl_2$ treatment ($P = 0.29$, t-test). In contrast to the findings regarding the WW leaflets, in the DA leaflets, both initial slopes of the A–C_i and A–C_c responses did not change after treatment with mercury ($P = 0.61$, t-test).

In the WW leaflets, g_i decreased by 30% when the mercury treatment was applied (Fig. 9). In contrast, in the DA leaflets, g_i was insensitive to the mercury treatment. After the mercury treatment, there was no significant difference in g_i between the WW and the DA leaflets. Similar results held true for changes in g_s.

To calculate g_i, we assumed that R_d was half of the dark respiration rate. To determine how much the g_i values change if R_d is lowered by the mercury treatment, we recalculated the g_i values of the mercury-treated leaflets assuming that R_d was one-tenth of the dark respiration rates. This results in an average g_i decrease of <5% in both the WW and DA leaflets. Changes in R_d did not significantly affect our g_i estimations.

Discussion

Effects of leaf anatomical characteristics and aquaporin activity on g_i

Our results suggest that the significant reductions in g_i in DA tobacco leaves did not result from leaf anatomical

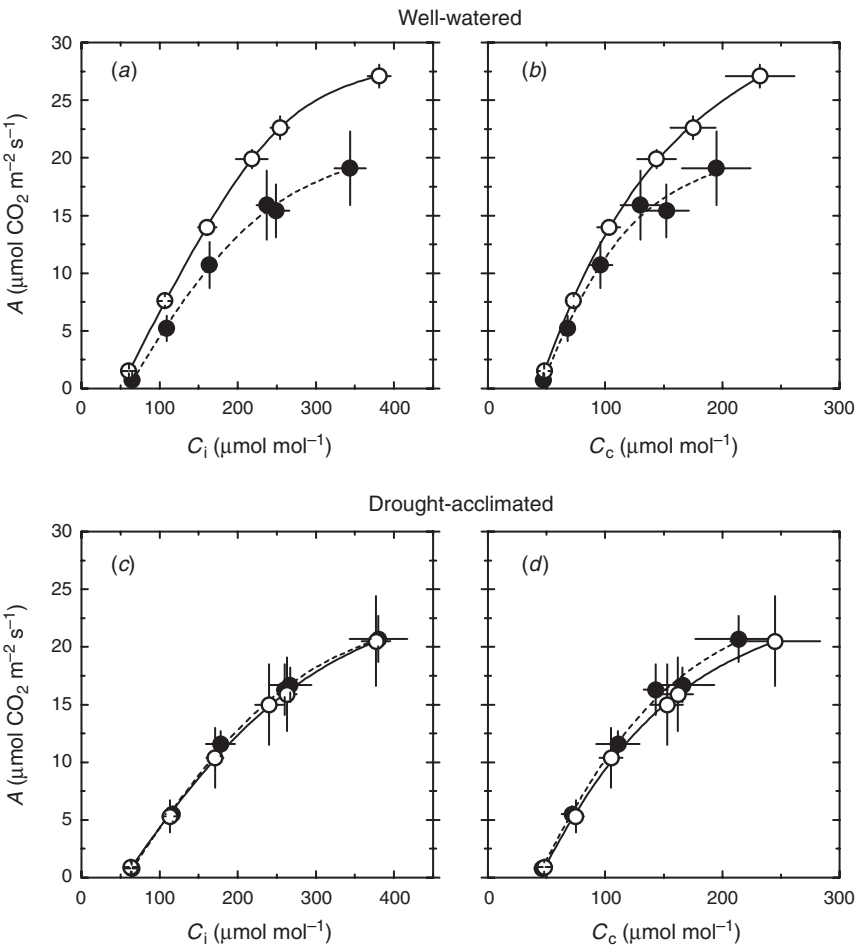

Fig. 8. Effects of $HgCl_2$ on A–C_i and A–C_c responses in (*a*, *b*) well-watered and (*c*, *d*) drought-acclimated tobacco plants. ○, responses before 0.5 mM $HgCl_2$ feeding; ●, responses after 0.5 mM $HgCl_2$ feeding. C_i and C_c indicate the CO_2 concentrations in the substomatal cavities and chloroplasts, respectively. C_c was calculated by the chlorophyll fluorescence method. Data are the mean ± s.d. of five and four sample leaflets for well-watered and drought-acclimated plants, respectively. Non-rectangular hyperbolic curves were fitted to the data.

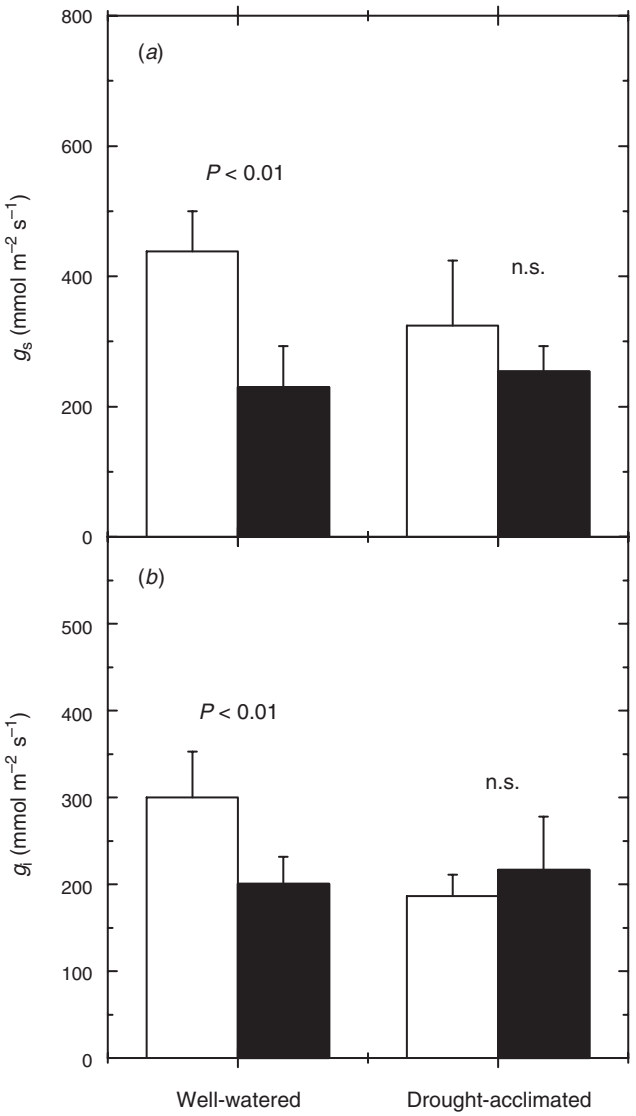

Fig. 9. Effects of $HgCl_2$ on stomatal conductance to water vapour (g_s) and internal conductance to CO_2 (g_i) in well-watered and drought-acclimated tobacco plants. Open bars, conductance before 0.5 mM $HgCl_2$ feeding; solid bars, conductance after 0.5 mM $HgCl_2$ feeding. g_s was measured under an ambient CO_2 concentration of 360 μmol mol^{-1}. g_i was calculated by the chlorophyll fluorescence method. Data are the mean ± s.d. of five and four sample leaflets for well-watered and drought-acclimated plants, respectively. For each treatment, *t*-tests were conducted before and after $HgCl_2$ feeding. n.s., not significant.

changes because S_c remained unchanged (Table 4). In addition, the gas-phase conductance to CO_2 (g_{gas}) in the DA leaves would be higher than that in the WW leaves because the mesophyll thickness decreased in response to the drought treatment (Fig. 4). S_c was retained because the decrease in the mesophyll surface area accompanied by the decrease in mesophyll thickness was compensated for by the high mesophyll cell density. We conclude that the significant reduction in g_i can be attributed to a decrease in the liquid-phase conductance per unit S_c (g'_{liq}).

Mercury binds the cysteine residues in the cytoplasmic sites of aquaporins thereby inhibiting water transport (Tazawa *et al*. 1996; Suga and Maeshima 2004). In the desert succulent *Agave deserti* Engelm., root hydraulic conductivity becomes insensitive to $HgCl_2$ treatment when the roots are grown under drought conditions (North and Nobel 2000). These researchers suggest that the aquaporin gating is closed by drought treatment, resulting in insensitivity of the root hydraulic conductivity to mercury. They also suggest that symplastic water transport via aquaporins becomes less important than apoplastic water transport in roots during long-term drought. Similarly, in tobacco, both g_i and water permeability in the DA leaves were insensitive to mercury treatment, whereas those in the WW leaves were markedly reduced by mercury treatment (Figs 7 and 9).

Stomatal conductance (g_s) in the DA leaves was lower than that in the WW leaves (Figs 3 and 9). The transpiration rate was monitored during $HgCl_2$ feeding (2.5–3.0 h), just before measurement of the second A–C_i response. The cumulative transpiration amount during the mercury treatment did not differ considerably between the treated leaflets (40 ± 6 mol m^{-2} (mean ± s.d.) for the WW leaflets and 33 ± 10 mol m^{-2} for the DA leaves). The magnitude of the decrease in g_i was independent of the cumulative transpiration amount, implying that the mercury insensitivity of g_i in the DA leaves did not result from a difference in the amount of mercury accumulated in their leaves.

A PIP1-type aquaporin identified in tobacco (NtAQP1) is insensitive to mercury (Biela *et al*. 1999). In contrast, the protein levels of the PIP2-type aquaporins (mercury-sensitive aquaporin isoforms) in the DA tobacco leaves were comparable to those in the WW leaves (Fig. 6). Phosphorylation of purified phospholamban decreases the electrophoretic mobility of the proteins in SDS–PAGE (Wegener and Jones 1984). As found for the DA leaves, the mobility of the PIP2s slightly increased, implying that the PIP2s are dephosphorylated and, hence, aquaporin gating is closed (Johansson *et al*. 1996, 1998). Consequently, our results suggest that the mercury insensitivity of g_i in the DA leaves is not caused by a lack of PIP2s, but rather by closed gating of PIP2s.

Relationship between g_i and aquaporin content

The variations in g_i were not clearly explained by the total plasma membrane aquaporin (all PIP) content on a leaf-area basis (Fig. 5). Immunohistological studies have revealed that PIPs are accumulated in the xylem parenchyma as well as in the spongy parenchyma in tobacco leaves (Otto and Kaldenhoff 2000) and in the phloem sieve elements and stomatal guard cells in spinach leaves (Fraysse *et al*. 2005). In tobacco, a recent study showed that the inner chloroplast membranes contain NtAQP1 and the chloroplast NtAQP1 considerably affects the leaf CO_2 transport, namely g_i (Uehlein *et al*. 2008). The obscure relationships between all PIP content and g_i might result from this heterogeneity in the aquaporins in the leaf tissues. Further studies are needed to determine which aquaporin isoform mainly contributes to CO_2 transport and to what extent leaf aquaporins regulate not only CO_2 transport, but also water transport.

Water permeability and water-use efficiency

The water permeability, (iFW – dFW)/iFW, at zero mercury levels in the DA leaves was slightly lower than that in the WW leaves (Fig. 7), but there was no statistical difference between the treatments ($P = 0.15$, *t*-test). The DA leaves had the lower iFW (perhaps owing to the reduced leaf thickness), but they had similar S_{mes} to the WW leaves (Fig. 7; Table 4). Therefore, when calculating water permeability as relative weight loss the water permeability of the DA leaves should be overestimated compared with the WW leaves. The absolute weight loss (i.e. iFW – dFW) in the DA leaves was 15% lower than that in the WW leaves. There was a modest significant difference in iFW – dFW between the treatments ($P = 0.06$, *t*-test), suggesting that the actual water permeability in the DA leaves is lower than that in the WW leaves.

In a leaf, water flows from the vascular vessels to the stomatal pores through two pathways: the mesophyll apoplastic and symplastic pathways (Jones 1992). The closed state of PIP2-type aquaporins in the mesophyll cells might reduce the water-flow via the symplastic pathway, which might decrease stomatal conductance and contribute to the increase in instantaneous WUE (Fig. 3).

Conclusions

In tobacco, the significant reduction in g_i in the DA leaves did not result from leaf anatomical changes. Our results suggest that mercury-sensitive aquaporins (PIP2s) are in a closed state in DA leaves and deactivation of the PIP2s leads to a significant reduction in g_i. Mesophyll CO_2 diffusion in the WW leaves is probably facilitated through the PIP2s, whereas diffusion in the DA leaves would be retarded by the closed gating of PIP2s.

Acknowledgements

S.-I. Miyazawa thanks Professor Ichiro Terashima for his constructive comments on early drafts of this manuscript and also Dr Hiroshi Yamamoto for his helpful suggestions. We also thank the anonymous reviewers for their advice. This work was supported by the Ministry of Economy, Trade and Industry (METI), Japan.

References

Atkin OK, Evans JR, Siebke K (1998) Relationship between the inhibition of leaf respiration by light and enhancement of leaf dark respiration following light treatment. *Australian Journal of Plant Physiology* **25**, 437–443.

Bernacchi CJ, Portis AR, Nakano H, von Caemmerer S, Long SP (2002) Temperature response of mesophyll conductance. Implications for the determination of Rubisco enzyme kinetics and for limitations to photosynthesis *in vivo*. *Plant Physiology* **130**, 1992–1998. doi: 10.1104/pp.008250

Biela A, Grote K, Otto B, Hoth S, Hedrich R, Kaldenhoff R (1999) The *Nicotiana tabacum* plasma membrane aquaporin NtAQP1 is mercury-insensitive and permeable for glycerol. *The Plant Journal* **18**, 565–570. doi: 10.1046/j.1365-313X.1999.00474.x

Chartzoulakis K, Patakas A, Kofidis G, Bosabalidis A, Nastou A (2002) Water stress affects leaf anatomy, gas exchange, water relations and growth of two avocado cultivars. *Scientia Horticulturae* **95**, 39–50. doi: 10.1016/S0304-4238(02)00016-X

Cooper GJ, Boron WF (1998) Effects of PCMBS on CO_2 permeability of *Xenopus* oocytes expressing aquaporin 1 or its C189S mutant. *The American Journal of Physiology* **275**, C1481–C1486.

Epron D, Godard D, Cornic G, Genty B (1995) Limitation of net CO_2 assimilation rate by internal resistances to CO_2 transfer in the leaves of two tree species (*Fagus sylvatica* L. and *Castanea sativa* Mill.). *Plant, Cell & Environment* **18**, 43–51. doi: 10.1111/j.1365-3040.1995.tb00542.x

Ethier GJ, Livingston NJ (2004) On the need to incorporate sensitivity to CO_2 transfer conductance into the Farquhar–von Caemmerer–Berry leaf photosynthesis model. *Plant, Cell & Environment* **27**, 137–153. doi: 10.1111/j.1365-3040.2004.01140.x

Evans JR, von Caemmerer S, Setchell BA, Hudson GS (1994) The relationship between CO_2 transfer conductance and leaf anatomy in transgenic tobacco with a reduced content of Rubisco. *Australian Journal of Plant Physiology* **21**, 475–495.

Flexas J, Ribas-Carbo M, Hanson DT, Bota J, Otto B, Cifre J, McDowell N, Medrano H, Kaldenhoff R (2006) Tobacco aquaporin NtAQP1 is involved in mesophyll conductance to CO_2 *in vivo*. *The Plant Journal* **48**, 427–439. doi: 10.1111/j.1365-313X.2006.02879.x

Flexas J, Ribas-Carbo M, Diaz-Espejo A, Galmes J, Medrano H (2008) Mesophyll conductance to CO_2: current knowledge and future prospects. *Plant, Cell & Environment* **31**, 602–621. doi: 10.1111/j.1365-3040.2007.01757.x

Fraysse LC, Wells B, McCann MC, Kjellbom P (2005) Specific plasma membrane aquaporins of the PIP1 subfamily are expressed in sieve elements and guard cells. *Biology of the Cell* **97**, 519–534. doi: 10.1042/BC20040122

Fredeen AL, Gamon JA, Field CB (1991) Responses of photosynthesis and carbohydrate-partitioning to limitations in nitrogen and water availability in field-grown sunflower. *Plant, Cell & Environment* **14**, 963–970. doi: 10.1111/j.1365-3040.1991.tb00966.x

Galmes J, Medrano H, Flexas J (2006) Acclimation of Rubisco specificity factor to drought in tobacco: discrepancies between *in vitro* and *in vivo* estimations. *Journal of Experimental Botany* **57**, 3659–3667. doi: 10.1093/jxb/erl113

Genty B, Briantais JM, Baker N (1989) The relationship between the quantum yield of photosynthetic electron transport and quenching of chlorophyll fluorescence. *Biochimica et Biophysica Acta* **990**, 87–92.

Hanba YT, Miyazawa S-I, Terashima I (1999) The Influence of leaf thickness on the CO_2 transfer conductance and leaf stable carbon isotope ratio for some evergreen tree species in Japanese warm-temperate forests. *Functional Ecology* **13**, 632–639. doi: 10.1046/j.1365-2435.1999.00364.x

Hanba YT, Shibasaka M, Hayashi Y, Hayasaka T, Kasamo K, Terashima I, Katsuhara M (2004) Overexpression of the barley aquaporin HvPIP2;1 increases internal CO_2 conductance and CO_2 assimilation in the leaves of transgenic rice plants. *Plant & Cell Physiology* **45**, 521–529. doi: 10.1093/pcp/pch070

Johanson U, Gustavsson S (2002) A new subfamily of major intrinsic proteins in plants. *Molecular Biology and Evolution* **19**, 456–461.

Johansson I, Larsson C, Ek B, Kjellbom P (1996) The major intrinsic proteins of spinach leaf plasma membranes are putative aquaporins and are phosphorylated in response to Ca^{2+} and apoplastic water potential. *The Plant Cell* **8**, 1181–1191. doi: 10.2307/3870361

Johansson I, Karlsson M, Shukla VK, Chrispeels MJ, Larsson C, Kjellbom P (1998) Water transport activity of the plasma membrane aquaporin PM28A is regulated by phosphorylation. *The Plant Cell* **10**, 451–459. doi: 10.2307/3870601

Jones HG (1992) 'Plants and Microclimate.' (Cambridge University Press: Cambridge)

Lambers H, Chapin FS III, Pons TL (1998) 'Plant Physiological Ecology.' (Springer-Verlag: New York)

Maeshima M (1992) Characterization of the major integral protein of vacuolar membrane. *Plant Physiology* **98**, 1248–1254.

Makino A, Mae T, Ohira K (1986) Colorimetric measurement of protein stained with Coomassie Brilliant Blue R on sodium dodecyl sulfate–polyacrylamide gel electrophoresis by eluting with formamide. *Agricultural and Biological Chemistry* **50**, 1911–1912.

Miyake C, Okamura M (2003) Cyclic electron flow within PSII protects PSII from its photoinhibition in thylakoid members from spinach chloroplasts. *Plant & Cell Physiology* **44**, 457–462. doi: 10.1093/pcp/pcg053

Miyazawa S-I, Terashima I (2001) Slow chloroplast development in the evergreen broad-leaved tree species: relationship between leaf anatomical characteristics and photosynthetic rate during leaf development. *Plant, Cell & Environment* **26**, 745–755.

Monti A, Brugnoli E, Scartazza A, Amaducci MT (2006) The effect of transient and continuous drought on yield, photosynthesis and carbon isotope discrimination in sugar beet (*Beta vulgaris* L.). *Journal of Experimental Botany* **57**, 1253–1262. doi: 10.1093/jxb/erj091

Nakhoul NL, Davis BA, Romero MF, Boron W (1998) Effect of expressing the water channel aquaporin-1 on the CO_2 permeability of *Xenopus* oocytes. *The American Journal of Physiology* **43**, C543–C548.

Nobel PS (1999) 'Physicochemical and Environmental Plant Physiology.' (Academic Press: San Diego)

North GB, Nobel PS (2000) Heterogeneity in water availability alters cellular development and hydraulic conductivity along roots of a desert succulent. *Annals of Botany* **85**, 247–255. doi: 10.1006/anbo.1999.1026

Ohshima Y, Iwasaki I, Suga S, Murakami M, Inoue K, Maeshima M (2001) Low aquaporin content and low osmotic water permeability of the plasma and vacuolar membranes of a CAM plant *Graptopetalum paraguayense*: comparison with radish. *Plant & Cell Physiology* **42**, 1119–1129. doi: 10.1093/pcp/pce141

Otto B, Kaldenhoff R (2000) Cell-specific expression of the mercury-insensitive plasma-membrane aquaporin NtAQP1 from *Nicotiana tabacum. Planta* **211**, 167–172. doi: 10.1007/s004250000275

Parkhurst DF, Mott KA (1990) Intercellular diffusion limits to CO_2 uptake in leaves. *Plant Physiology* **94**, 1024–1032.

Porra RJ, Thompson WA, Kriedemann PE (1989) Determination of accurate extinction coefficients and simultaneous equations for assaying chlorophyll *a* and *b* extracted with four different solvents: verification of the concentration of chlorophyll standards by atomic absorption spectroscopy. *Biochimica et Biophysica Acta* **975**, 384–394. doi: 10.1016/S0005-2728(89)80347-0

Reich PB, Walters MB, Tabone TJ (1989) Response of *Ulmus americana* seedlings to varying nitrogen and water status. 2 Water and nitrogen use efficiency in photosynthesis. *Tree Physiology* **5**, 173–184.

Suga S, Maeshima M (2004) Water channel activity of radish plasma membrane aquaporins heterologously expressed in yeast and their modification by site-directed mutagenesis. *Plant & Cell Physiology* **45**, 823–830. doi: 10.1093/pcp/pch120

Suga S, Imagawa S, Maeshima M (2001) Specificity of the accumulation of mRNAs and proteins of the plasma membrane and tonoplast aquaporins in radish organs. *Planta* **212**, 294–304. doi: 10.1007/s004250000396

Syvertsen JP, Lloyd J, McConchie C, Kriedemann PE, Farquhar GD (1995) On the relationship between leaf anatomy and CO_2 diffusion through the mesophyll of hypostomatous leaves. *Plant, Cell & Environment* **18**, 149–157. doi: 10.1111/j.1365-3040.1995.tb00348.x

Tazawa M, Asai K, Iwasaki N (1996) Characteristics of Hg- and Zn-sensitive water channels in the plasma membrane of *Chara* cells. *Botanica Acta* **109**, 388–396.

Terashima I, Ono K (2002) Effects of $HgCl_2$ on CO_2 dependence of leaf photosynthesis: evidence indicating involvement of aquaporins in CO_2 diffusion across the plasma membrane. *Plant & Cell Physiology* **43**, 70–78. doi: 10.1093/pcp/pcf001

Terashima I, Miyazawa S-I, Hanba YT (2001) Why are sun leaves thicker than shade leaves? Consideration based on analyses of CO_2 diffusion in the leaf. *Journal of Plant Research* **114**, 93–105. doi: 10.1007/PL00013972

Terashima I, Araya T, Miyazawa S-I, Sone K, Yano S (2005) Construction and maintenance of the optimal photosynthetic systems of the leaf, herbaceous plant and tree: an eco-developmental treatise. *Annals of Botany* **95**, 507–519. doi: 10.1093/aob/mci049

Thain JF (1983) Curvature correction factors in the measurement of cell surface areas in plant tissues. *Journal of Experimental Botany* **34**, 87–94. doi: 10.1093/jxb/34.1.87

Uehlein N, Lovisolo C, Siefritz F, Kaldenhoff R (2003) The tobacco aquaporin NtAQP1 is a membrane CO_2 pore with physiological functions. *Nature* **425**, 734–737. doi: 10.1038/nature02027

Uehlein N, Otto B, Hanson DT, Fischer M, McDowell N, Kaldenhoff R (2008) Function of *Nicotiana tabacum* aquaporins as chloroplast gas pores challenges the concept of membrane CO_2 permeability. *The Plant Cell* **20**, 648–657. doi: 10.1105/tpc.107.054023

von Caemmerer S (2000) 'Biochemical models of leaf photosynthesis.' (CSIRO Publishing: Collingwood)

Warren CR (2008) Soil water deficits decrease the internal conductance to CO_2 transfer but atmospheric water deficits do not. *Journal of Experimental Botany* **59**, 327–334. doi: 10.1093/jxb/erm314

Wegener AD, Jones LR (1984) Phosphorylation-induced mobility shift in phospholamban in sodium-dodecyl-sulfate–polyacrylamide gels. *Journal of Biological Chemistry* **259**, 1834–1841.

Yamori W, Noguchi K, Hanba YT, Terashima I (2006) Effects of internal conductance on the temperature dependence of the photosynthetic rate in spinach leaves from contrasting growth temperatures. *Plant & Cell Physiology* **47**, 1069–1080. doi: 10.1093/pcp/pcj077

Yang B, Fukuda N, van Hoek A, Matthay MA, Ma T, Verkman AS (2000) Carbon dioxide permeability of aquaporin-1 measured in erythrocytes and lung of aquaporin-1 nul mice and in reconstituted proteoliposomes. *Journal of Biological Chemistry* **275**, 2686–2692. doi: 10.1074/jbc.275.4.2686

Manuscript received 10 April 2008, accepted 3 June 2008